Oncogene (2002) 21, 4435–4447

www.nature.com/onc

CL100 expression is down-regulated in advanced epithelial ovarian cancer and its re-expression decreases its malignant potential

Ramon G Manzano[1], Luis M Montuenga[1,5], Mark Dayton[2], Paul Dent[3], Ichiro Kinoshita[1], Silvestre Vicent[1,5], Ginger J Gardner[1], PhuongMai Nguyen[1], Yung-Hyun Choi[1], Jane Trepel[1], Nelly Auersperg[4] and Michael J Birrer*[,1]

[1]*Cell and Cancer Biology Department, National Cancer Institute, 9610 Medical Center Drive, Rockville, Maryland, MD 20850, USA;* [2]*Department of Medicine, Louisiana State University Medical Center, Shreveport, Louisiana, LA 71130-3932, USA;* [3]*Department of Radiation Oncology, Massey Cancer Center, Medical College of Virginia, Virginia Commonwealth University, Richmond, Virginia, VA 23298, USA;* [4]*Department of Obstetrics and Gynecology, University of British Columbia, Vancouver, British Columbia Canada V6H 3V5*

Although early stage ovarian cancer can be effectively treated with surgery and chemotherapy, the majority of cases present with advanced disease, which remains essentially incurable. Unfortunately, little is known about the genes important for the development and progression of this disease. In this study, the expression of 68 phosphatases was determined in immortalized ovarian epithelial cells (IOSE) and compared to ovarian cancer cell lines. CL100, a dual specificity phosphatase, displayed 10–25-fold higher expression in normal compared to malignant ovarian cell lines. Immunohistochemical staining of normal ovaries and 68 ovarian cancer specimens confirmed this differential expression. Re-expression of CL100 in ovarian cancer cells decreased adherent and non-adherent cell growth and induced phenotypic changes including loss of filopodia and lamellipodia with an associated decrease in cell motility. Induced expression of CL100 in ovarian cancer cells suppressed intraperitoneal tumor growth in nude mice. These results show for the first time that CL100 expression is altered in human ovarian cancer, that CL100 expression changes cell morphology and motility, and that it suppresses intraperitoneal growth of human ovarian epithelial cancer. These data suggest that down-regulation of CL100 may play a role in the progression of human ovarian cancer.
Oncogene (2002) **21,** 4435–4447. doi:10.1038/sj.onc.1205542

Keywords: MKP-1; ovarian; cancer; phosphatases; growth; motility

Introduction

Epithelial ovarian cancer is the fifth leading cause of cancer mortality in women in the United States. In 2001, there will be an estimated 23 400 new cases of ovarian cancer which will result in approximately 13 900 deaths, making ovarian cancer second among gynecologic cancers in incidence and the most lethal of the gynecologic malignancies (Greenlee *et al*., 2001). The five-year survival of patients diagnosed with ovarian cancer is approximately 30% and has not changed appreciably over the past 30 years despite important advances in surgery, radiation and chemotherapy (Devesa *et al*., 1995). This emphasizes the need for new therapies based upon a greater understanding of the molecular mechanisms underlying ovarian carcinoma. Recent efforts to characterize genetic alterations in epithelial ovarian cancer have revealed extensive cytogenetic and molecular alterations in these tumors (Cliby *et al*., 1993; Dodson *et al*., 1993). However, very little is known about the basic molecular mechanisms that deregulate the growth of the ovarian epithelium and lead to invasive and metastatic behavior of these tumors. To design rational treatments, the genes involved in the development and progression of ovarian cancer must be identified.

In eukaryotic cells, there is a balance between the activity of protein tyrosine kinases (PTKs) and protein tyrosine phosphatases (PTPs) for the control of different physiologic processes such as growth, differentiation, and motility (Tonks and Neel, 1996; Neel and Tonks, 1997). Malignant transformation can occur when this balance is disturbed, either by an increased activity of PTKs or by a decreased activity of PTPs (Tonks and Neel, 1996; Neel and Tonks, 1997). PTKs have been considered key molecules in the phosphorylation of tyrosine residues in a variety of proteins (Tonks and Neel, 1996), but in recent years more attention is directed to the growing number of PTPs. Although, genome sequencing data predict the existence of approximately 500 human

*Correspondence: MJ Birrer; E-mail: birrerm@bprb.nci.nih.gov
[5]Current address: Cytology and Histology Department, University of Navarra, Pamplona, Spain
Received 3 December 2001; revised 27 March 2002; accepted 2 April 2002

PTPs (Neel and Tonks, 1997), their physiological relevance is not yet well understood. PTPs are characterized by at least a catalytic domain containing a unique 'signature motif' (Neel and Tonks, 1997), and several families of PTPs have been described: transmembrane receptor-like PTPs, non-receptor non-transmembrane PTPs, dual-specificity phosphatases (DSPs) and low molecular weight phosphatases. A variety of biological functions have been assigned to these PTPs, including a possible role as tumor suppressor genes for some PTPs (Fischer *et al*., 1991). In an attempt to evaluate a potential role of protein tyrosine phosphatases (PTPs) in human epithelial ovarian cancer, we determined the differential expression of 68 different PTPs by RT–PCR in a panel of human ovarian cancer cell lines compared to normal ovarian cell surface epithelium immortalized with the SV-40 large-T antigen (Maines-Bandiera *et al*., 1992). CL100, the human homolog of Mitogen-Activated Protein Kinase Phosphatase 1 (MKP-1) is downregulated in ovarian cancer versus normal immortalized cell lines. This report characterizes the role of CL100 in ovarian cancer.

Results

Differential expression of CL100 in IOSEs versus malignant ovarian cell lines

By using specific pairs of primers for different phosphatases, patterns of relative expression of 68 phosphatases were identified in IOSE cells (Maines-Bandiera *et al*., 1992), and these results were compared to the expression patterns found in tumor cell lines (Table 1), as it was hypothesized that differences in phosphatase expression between IOSEs and cancer cells might be important for the biology of ovarian cancer.

CL100, a dual specificity phosphatase (DSP), was analysed further because it had high expression in IOSEs and very low expression in ovarian cancer cell lines. Other DSPs including those belonging to the same family of MAPK phosphatases (such as MKP-2 and MKP-3) were not differentially expressed. The expression of CL100 was quantitated in a panel of 16 human ovarian cell lines by Northern blot (Figure 1a). High expression of CL100 was observed in the two IOSE cell lines. Twelve out of 14 tumor cell lines (86%) showed less than 13% of CL100 expression (average 7%) compared to the IOSE cell lines, including no detectable expression in OVT2 cells. Cell line A224 expressed a similar level of CL100 as the IOSE cells while tumor cell line A364 expressed 40%. As immortalization with T-antigen could lead to alterations in gene expression in normal ovarian cells, we compared the expression of CL100 in low passage normal human ovarian surface epithelium (HOSE) cells to that in IOSE 80 and IOSE 120. High CL100 expression was also found in HOSE cells (Figure 1b).

Table 1 Expression level of phosphatases in immortalized ovarian epithelial cells

High	*Intermediate-High*	*Intermediate-Low*	*Low*
LAR	PTP-TD14	PTPψ	rOST-PTP
PTPα	PTPκ	rBEM-2	PTPϕ
SHP-2	PTPη	PTPγ[a]	PTPζS
PEZ	SAP-1	PTPεC	PTPζL
PTP-1Bα	PTPσP1	PTPδ	rPTPσPS
PEST	PTPμ	LCA	HePTPase
PTPmeg2	PTPβ[a]	PTPζ	SHP1
PTP-BASab	PTPεM	PTP-BR7	PTP-BAS3E
PTP-1B	PTP-H1	PTP-1Bb	STEP
MTMR1	PTP-D1	PTP-BAS4E	Mptp-HSCF
MTMR2	TC-PTP	PTP-BASc	PTP-BAS2E
MTMR3	TC-PTPa	BDP1	mIA-2β
VHR	PTP-BASa	PEP	ICAAR
VH-3	PTPmeg01	PTP-BAS5E	PDSP2
CL100[a]	TC-PTPb	PTP-BAS23E	
Cdc25b[a]	PTP-BASb	IA2	
HCa	MTM1	MAPKP-4	
PRL-CAAX2	MMAC1/PTEN	PRL-CAAX3	
PDSP4	MKP-X	PDSPinh	
	KAP-1	mPDSP1	
	VH-5	PDSP6	
	PIR1	PDSP5	
	MKP-3	mPDSP3	
	MKP-2		
	Cdc 25a		
	Cdc25c[a]		
	HCb		
	PRL-CAAX1		
	STYXb		

[a]Indicates the only phosphatases that were differentially expressed in normal versus cancer cell lines. The rest of phosphatases were not differentially expressed. A two tailed student *t*-test was carried out with the average expression values obtained from the RT–PCR analysis of two normal immortalized ovarian cell lines and three ovarian cancer cell lines as described in (Devesa *et al*., 1995; Dodson *et al*., 1993). The [a] indicates $P \leqslant 0.05$ (*t*-test, two tailed)

Decreased CL100 expression in ovarian cancer specimens compared to normal ovarian epithelium

To determine whether CL100 expression was decreased in primary ovarian cancer, 68 surgically resected primary epithelial ovarian carcinomas and 10 normal ovaries were immunohistochemically stained utilizing a polyclonal antibody specific for MKP-1 (Santa Cruz Biotechnology). The A224 cell line served as a positive control and demonstrated intense nuclear staining with minimal cytoplasmic staining (Figure 2a,b). Nine out of 10 normal ovaries scored positive for nuclear staining of the surface epithelial layer (Figure 2c,d). Thirty-five per cent of tumors retained CL100 expression (Figure 2e–h and Table 2) and the difference between normal and tumor samples was statistically significant ($P = 0.001$ by Fisher's exact test). Furthermore, immunostaining of the ovarian carcinoma samples demonstrated a progressive loss of CL100 expression from early to late stage disease (Figure 2e–h). Advanced tumors (stages III and IV) revealed minimally detectable staining and the negative correlation between CL100 expression and the pathological stage was significant (stage I and II versus stages III and IV; $P < 0.001$ chi-squared test). Since histologic

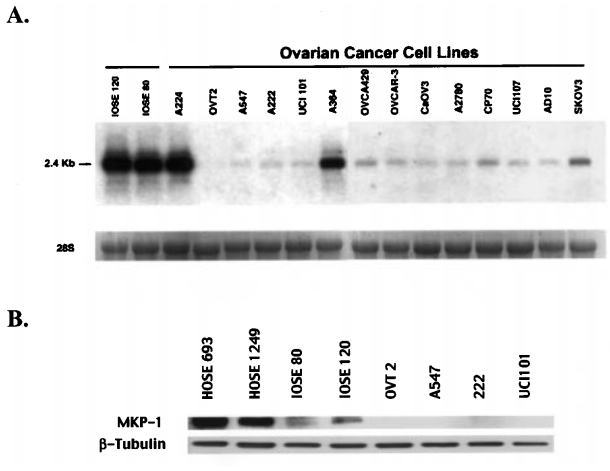

Figure 1 (**a**) Northern blot showing CL100 expression in immortalized and malignant ovarian cell lines. 28S RNA is shown as loading control. Cells were collected in exponential growth from subconfluent cultures and were processed as indicated in the Materials and methods section. (**b**) Western blot using HOSE cells and IOSE cells (5 μg of total protein was loaded). The same membrane was probed with an anti-tubulin antibody, used as loading control

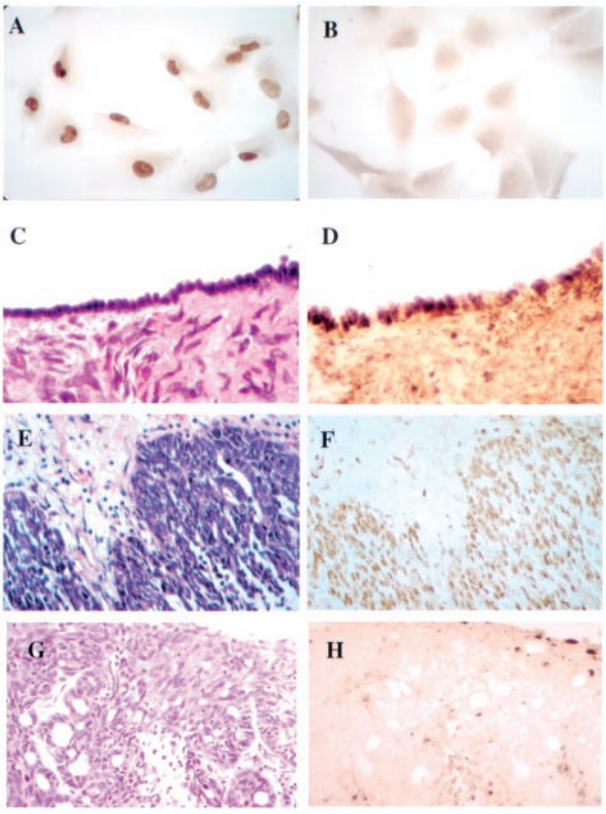

Figure 2 Expression of CL100 in ovarian tissues and tumors. (**a**) Immunohistochemical staining of the ovarian cancer cell line A224 (which displays high constitutive expression of CL100, see Figure 1) with a rabbit polyclonal antibody against MKP-1. Nuclear staining is evident. (**b**) The same cell line stained with an IgG isotype matched control antibody. No nuclear staining can be seen. (**c**) H and E staining of normal ovarian surface epithelial cells. (**d**) Immunohistochemical staining of the same ovarian surface epithelial layer for CL100. (**e**) H and E staining of an early stage papillary serous ovarian adenocarcinoma. (**f**) Immunohistochemical staining of the same tumor (E) for CL100. (**g**) H and E staining of an advanced stage papillary serous ovarian adenocarcinoma. (**h**) Immunohistochemical staining of the same tumor (G) for CL100

subtypes demonstrated different staining rates, we analysed the relationship between stage and staining within histologic subgroup. The only subgroup that had sufficient numbers to analyse were serous tumors, which demonstrated a statistically significant difference between early and late stage ($P<0.05$ by Fisher exact test). The degree of differentiation did not correlate with CL100 expression.

As CL100 is inducible by different types of oxidative stress (Keyse and Emslie, 1992), the CL100 RNA expression in several ovarian cancer cell lines was evaluated under oxidative stress. Hydrogen peroxide (Figure 3) can increase CL100 RNA levels up to 15-fold within 2 h of treatment with these oxidants and remained elevated for up to 6 h. Cell lines with low baseline expression of CL100 (A2780 and UCI101) (Figure 3) responded to oxidative stress, suggesting that normal regulation of CL100 by oxidative stress does occur in ovarian tumor cell lines. However, OVT2 cells which display an abnormal CL100 genomic structure, also failed to exhibit CL100 inducibility by oxidative stress (Figure 3).

Re-expression of CL100 in ovarian cancer cells decreases anchorage dependent and independent growth

The biologic role of decreased expression of CL100 in ovarian cancer was assessed by reexpressing it in two ovarian cancer cell lines (A2780 and UCI101) possessing low endogenous levels of CL100. In addition to having low endogenous levels of CL100, these cell lines were chosen because they are easy to transfect and have a high growth rate. Individual clones with stable expression of CL100 as well as control clones in A2780 and UCI101 cells (Figure 4a) were isolated. The clones isolated from A2780 (AL3, AL8, AL18 and AL21) and UCI101 (UL2, UL11, UL12, and UL13) had CL100 protein levels, which were lower than those of the IOSEs (not shown). Analysis of the subcellular localization of CL100 in some of these transfectants revealed that the majority of the protein localized to the nucleus (Figure 4b). To assess whether the CL100 construct used was enzymatically active, quantitation of MAP kinase activities in two of the CL100 expressing clones (AL18 and AL21) as well as in two matched vector control clones (AC1 and AC3) randomly chosen was performed. Decreased ERK-2 and JNK-1 but not p38 kinase activities as compared to control clones was observed (Figure 4c), proving that indeed the construct used is active. Analysis of cellular proliferation revealed that CL100 transfected clones in A2780 and UCI101 cells had a slower growth rate than control clones (Figure 4d). There were no

Table 2 CL100 expression in primary ovarian specimens

		Number of patients	*Positive staining %*	
Histology				
	Normal	10	9/10	(90)
	Cancers	50	21/50	(42)
	Serous	24	6/24	(25)
	Mucinous	6	5/6	(83.3)
	Clear cell	8	7/8	(87.5)
	Endometrioid	11	3/11	(27.2)
	Others	1	0/1	(0)
Stage				
	I	23	14/23	(60.8)
	II	9	6/9	(66.6)
	III	18	1/18	(5.5)
Differentiation				
	G1	8	5/8	(62.5)
	G2	6	3/6	(50)
	G3	29	9/29	(31)

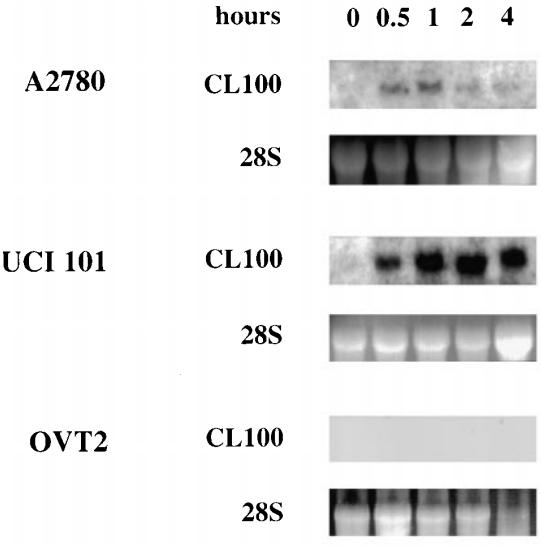

Figure 3 Induction of CL100 by hydrogen peroxide. Cells (A2780, UCI 101 and OVT2) were treated for half an hour with 200 μM H_2O_2 and then collected at the indicated time points and analysed by Northern blot for CL100 expression

morphological signs of apoptosis in the cells over-expressing CL100. CL100 expressing cell lines also had a decreased ability to form colonies in soft agar as compared with the vector control cells (Figure 4e).

CL100 expression decreases lamellipodia, filopodia and cellular motility

To analyse the biological effects of CL100 in more detail and eliminate potential problems from clonal variation, we generated three UCI101 clones with conditional expression of CL100 (U8 and U28) using an amphotrophic retrovirus (Watsuji *et al*., 1997) expressing CL100 under the control of a tetracycline regulated promoter (rtTA, tet on system). The addition of doxycycline (1 μg/ml) to the culture medium induced expression of CL100 after 48 h (20-fold increased) (Figure 5a), producing CL100 expression levels comparable to those found in IOSE cells. The addition of the same concentration of doxycycline to a control clone (U30) did not induce expression of CL100 (Figure 5a).

Under induction with doxycycline, all three UCI101 clones demonstrated reversible phenotypic changes by the third day. Cells with conditional expression of CL100 were flattened, enlarged and rounded compared with uninduced cells or with U30+ cells, which had a spindle-like morphology (Figure 5b). Induced cells formed tight clusters, whereas uninduced cells (and control clone U30) demonstrated close contact with each other only upon confluence. A more detailed characterization utilizing scanning electron microscopy (s.e.m.) revealed a loss of filopodia and lamellipodia at the leading edge of U28+ cells but not U30+ (Figure 6a). This result was confirmed by staining for F-actin fibers, which revealed that lamellipodia and filopodia present in U28− are decreased after CL100 induction (Figure 6b). Since the morphological changes induced by CL100 involve structures that are known to be important for cell movement, cellular motility was assayed. U28+ were less motile than the U28− cells *in vitro* while the motility of the U30 clone was not significantly different either in the presence or in the absence of doxycycline (Figure 6c, $P=0.00008$ student *t*-test).

CL100 decreases cyclin D1 expression

Since cyclin D1 has been demonstrated to be important in the progression of the cell cycle mediated by growth factor-induced MAPK pathways, the effect of CL100 on the expression of cyclin D1 was determined. Decreased cyclin D1 protein expression was observed in U28 upon induction with doxycycline (Figure 7a). Similar results were obtained with U8 (data not shown). Cotransfection of CL100 and a luciferase reporter under the control of a 1.7 Kb fragment of the cyclin D1 promoter demonstrated decreased reporter activity in UCI 101 and A2780 parental cell lines (Figure 7b), showing that transient expression of CL100 can regulate cyclin D1 transcriptional activity in these cell lines. Further analysis using shorter cyclin D1 promoter constructs with deletion mutants of single known consensus binding sites for different transcription factors revealed that the downregulation of the cyclin D1 reporter activity mediated by CL100 maps to an AP1 site present at −947 bp (Figure 7c). The decreased reporter activity induced by transfection of CL100 is abolished by using a deletion mutant of this AP1 site in the cyclin D1 promoter.

CL100 expression suppresses intraperitoneal tumor growth in nude mice

To test the *in vivo* relevance of CL100 expression in ovarian cancer cells, tumor formation in nude mice was studied (Table 3). Two different cell lines with

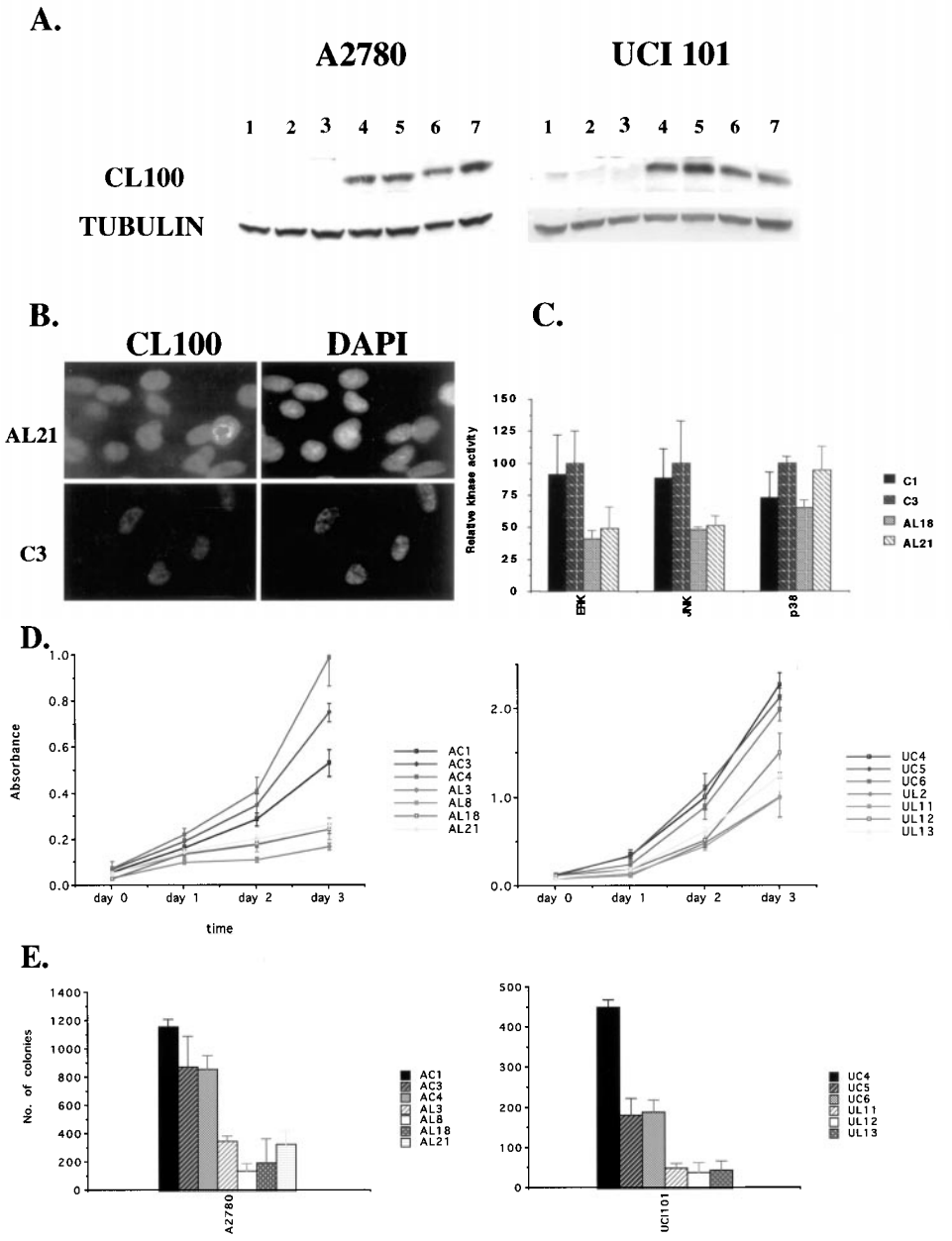

Figure 4 (**a**) Western blot of A2780 stable transfectants. (1) C1, (2) C3 and (3) C4. 1,2 and 3 are control A2780 clones stably transfected with pcDNA3; (4) AL3 (5) AL8 (6) AL18 and (7) AL21. Four to seven are A2780 clones stably transfected with pcDNA3-CL100. Western blot of UCI101 stable transfectants: (1) UC4 (2) UC5 (3) UC6. One to three are control UCI101 clones stably transfected with pcDNA3; (4) UL2 (5) UL11 (6) UL12 (7) UL13. Four to seven are UCI101 clones stably transfected with pcDNA3-CL100. β-tubulin is used as a loading control on the same membranes. (**b**) Subcellular localization of CL100 in AL21 and C3 (A2780 stable transfectants) by immunofluorescence as described in the Materials and methods section. (**c**) ERK-2, JNK-1 and p38 kinase activities of A2780 CL100 transfectants (AL18 and AL21) versus A2780 transfected with empty vector alone (C1 and C3). The results are expressed as percentage of control, and were measured in fmol/min/mg of protein, and are the mean and s.d. of three independent experiments. Comparison of the kinase activity in control clones to CL100 expressing clones demonstrated a statistically signficant difference for ERK and JNK ($P<0.05$) but not p38. (**d**) Cell proliferation as measured by a MTT colorimetric assay of A2780 control clones (C1, C3 and C4) and A2780 cells overexpressing CL100 (AL3, AL8, AL18 and AL21). Cell proliferation as measured by MTT colorimetric assay of UCI101 control clones (UC4, UC5 and UC6) and UCI101 cells overexpressing CL100 (UL2, UL11, UL12, and UL13) is also shown. Each time point is the mean and standard deviation of eight values. At three days, CL100 transfected clones in A2780 and UCI101 cells had a slower growth rate than control clones ($P<0.05$). (**e**) Number of colonies formed in soft agar by A2780 and UCI101 stable transfectants. CL100 expressing cell lines had a decreased ability to form colonies in soft agar compared with vector control cells ($P<0.05$). Each graph shows the results of a representative experiment out of three performed showing similar results. For each experiment each cell line was done in triplicate as described in the Materials and methods section

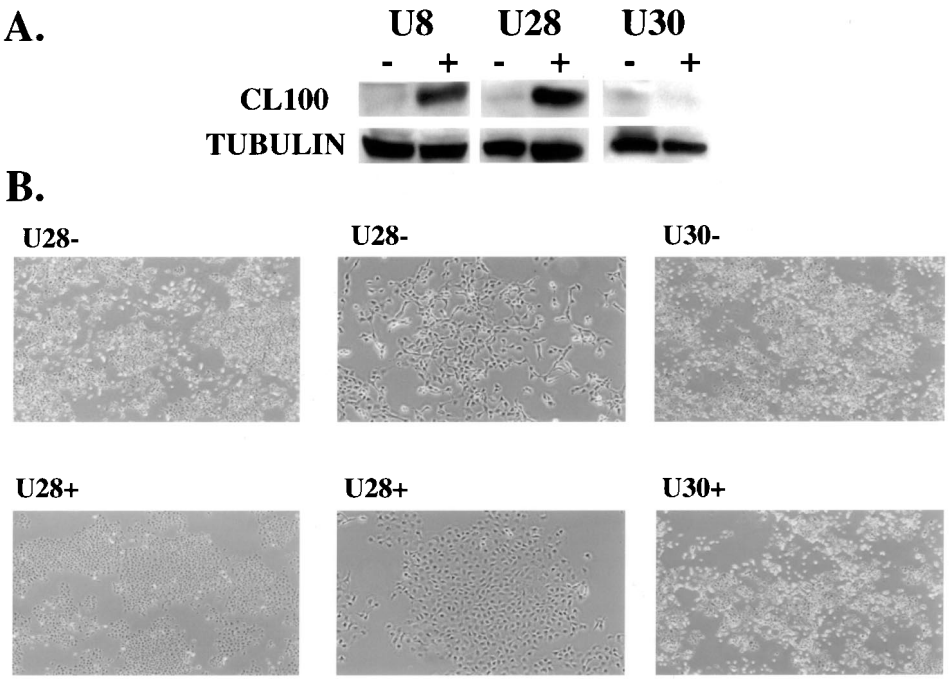

Figure 5 (**a**) Western blot of UCI101 inducible clones U8 and U28, in the absence (−) or presence (+) of doxycycline 1 μg/ml for 48 h. U30 represents a UCI101 clone that was infected with the same retrovirus but did not express CL100 upon induction with doxycycline. β-tubulin was used as a loading control in the same membranes. (**b**) Phase contrast microscopy showing the phenotypic changes induced by conditional expression of CL100 in U28 (magnifications: 20× and 40×) and U30 (magnification: 20×). Cells were plated in 100 mm dishes either in the presence (U28+ and U30+) or absence (U28− and U30−) of doxycycline for 5 days

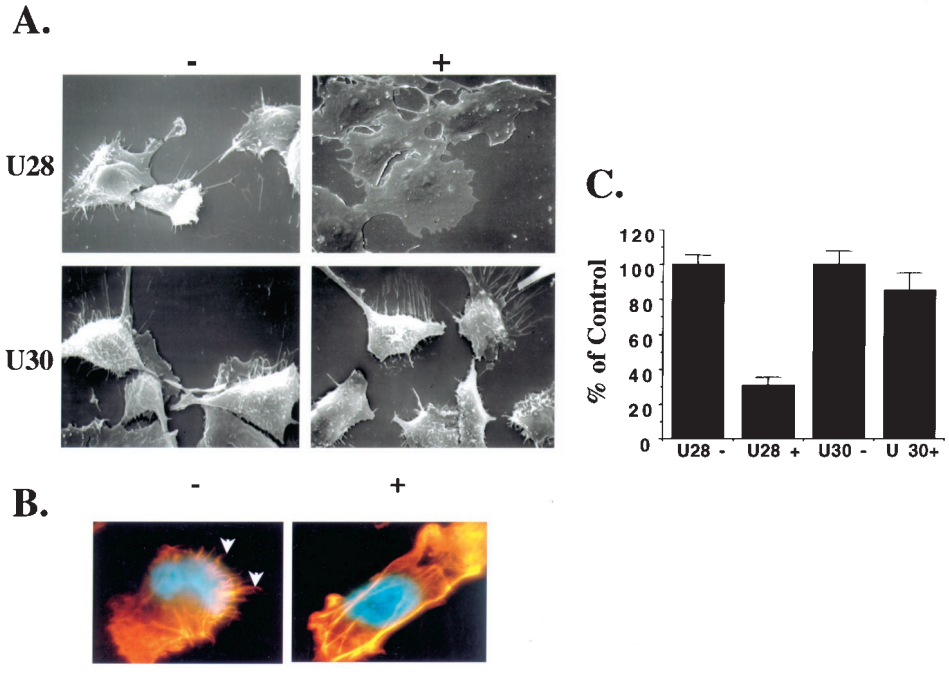

Figure 6 (**a**) Scanning electron microscopy showing the phenotypic changes induced by the conditional expression of CL100 in U28 but not in U30. (**b**) Staining of F-actin fiber in U28− and U28+ cells (63× magnification). DAPI and F-actin fibers staining was performed as described in Materials and methods. Arrows point to filopodia in U28− cells. (**c**) Motility of inducible clone U28 as compared to control clone U30. U28+ were significantly less motile than the U28− cells ($P=0.00008$); whereas, the U30 clone was not significantly different in the presence or absence of doxycycline. The experiment was carried out as described in the Materials and methods section. This figure shows one representative experiment (done in duplicate) out of three performed, obtaining similar results

conditional expression of CL100 were used: U28 (described above) and M18, which was obtained after selection of A2780 ovarian carcinoma cells infected with the pLRT-CL100 retrovirus. Since ovarian cancer is primarily an intraperitoneal disease, sets of animals were injected intraperitoneally as well as the more standard subcutaneous location. Two independent experiments were carried out. The first experiment included 10 mice per cell line for the subcutaneous location, and five per cell line for the intraperitoneal location. Subcutaneous tumors were not significantly different in any of the other cell lines used (U28− and + and M18− and +). However, the size of the peritoneal tumors was suppressed in the cells with conditional expression of CL100 (U28+ and M18+) in comparison with the uninduced controls (U28− and M18− respectively). This suppression reached statistical significance in M18 cells ($P=0.007$, *t*-test) and a clear trend was also observed in U28+ cells although it did not reach statistically significance ($P=0.06$, *t*-test). This lack of statistical significance was considered to be the result of having an insufficient number of mice for the U28 cell line. Therefore, a second experiment was carried out with a larger number of mice for the intraperitoneal location (Table 3). Two goals were pursued: first, to test the reproducibility of the intraperitoneal effects found in M18+, and secondly because it was estimated that the new number of mice used in the second experiment would be sufficient to achieve statistical significance in the U28+ cells. Again, in the second experiment, mice with doxycycline pellets have smaller peritoneal tumors than those with placebo pellets in both cell lines: M18 ($P=0.000$, *t*-test) and U28 ($P=0.011$, *t*-test), whereas the subcutaneous tumors (included as a control) were not statistically different in any of the cell lines. It was also noteworthy that U28− mice presented ascites more often than U28+ mice ($P=0.008$, Fisher exact test), indicating a more aggressive behavior in U28− as compared to U28+. Immunohistochemical analysis with a specific anti-MKP1 antibody of the tumors removed from nude mice showed that expression of CL100 was present at similar levels in both subcutaneous and intraperitoneal tumors formed by M18+ cells (Figure 8). Expression of CL100 was decreased and it presented a heterogeneous pattern in subcutaneous versus intraperitoneal tumors formed by the U28+ cells (Figure 8). Therefore, in M18 cells expression of CL100 did not suppress subcutaneous growth but in U28 a decreased expression of CL100 in the subcutaneous tumors could account, at least partially, for the lack of a growth inhibition in the subcutaneous location in this cell line.

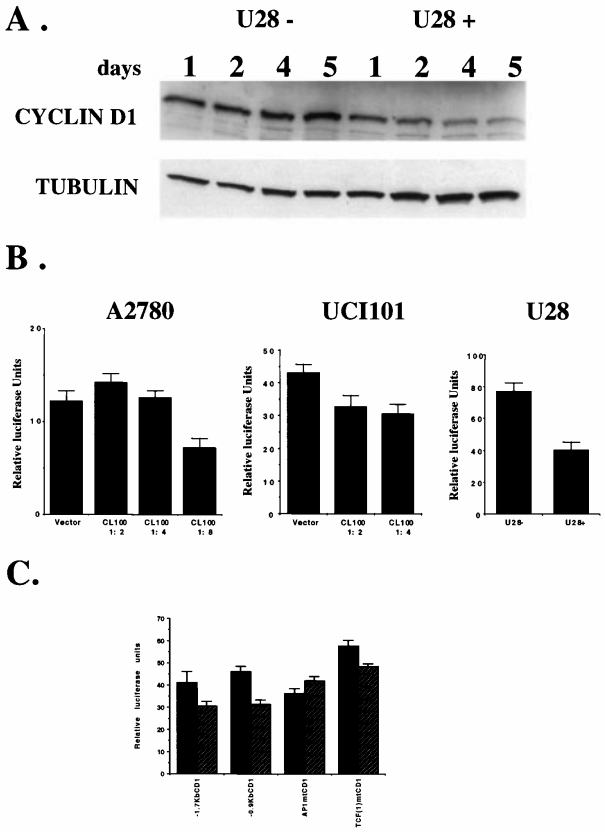

Figure 7 (**a**) Western blot of U28 cells in the absence (U28−) or in the presence (U28+) of doxycycline for the indicated time points using a cyclin D1 antibody (20 μg of protein per lane was loaded). The same membranes were probed sequentially with an anti β-tubulin antibody. (**b**) Luciferase reporter assays with a −1.7 Kb cyclin D1 promoter fragment as described in (Tetsu and McCormick, 1999). The amount of reporter construct used was 1 μg along with different proportions of pcDNA3-CL100 and 10 ng of renilla as control of transfection efficiency. One representative experiment done in triplicate is shown out of three performed in the parental ovarian cancer cell lines A2780 and UCI 101 as well as in the inducible U28 after 5 days of induction with doxycycline. A statistically significant decrease in reporter activity compared to empty vector controls was seen in A2780 cells transfected with CL100 1 : 8, UCI101 cells transfected with CL100 1 : 2 and 1 : 4, and U28+ cells compared to U28− ($P<0.05$). (**c**) Luciferase reporter assay with a 1.7 Kb, 0.9 Kb and a TCF and an AP1 deletion mutants of the human cyclin D1 promoter in UCI101 ovarian cancer cells. Solid bars indicate reporter values of vector alone transfected cells. Striped bars indicate reporter values of promoter construct transfected cells. Decreased reporter activity induced by the transfection of CL100 is abolished by using a deletion mutant of this AP1 site in the cyclin D1 promoter ($P<0.05$)

Discussion

The recent identification of phosphatases in the regulation of important signaling pathways implicated in cancer prompted us to characterize their specific patterns of expression in IOSE cells in comparison with ovarian cancer cell lines. Utilizing a semiquantitative RT–PCR assay provided us with a unique approach to broadly screen for the differential expression of phosphatases in ovarian specimens. This report presents a systematic screening to identify potentially relevant phosphatases involved in ovarian cancer biology. There is only one previous study analysing phosphatases in human ovarian cancer cells transfected with HER-2/neu (Wiener *et al*., 1996). We found that

Table 3 CL100 suppresses intraperitoneal but not subcutaneous tumor growth

	Subcutaneous (grams)		*Intraperitoneal (grams)*	*(ascites)*		
Cell line	*Exp. 1 (n=10)*	*Exp. 2 (n=5)*	*Exp. 1 (n=5)*	*Exp. 2 (n=9)*	*Exp. 1*	*Exp. 2*
U28−	1.10±1.70	0.22±0.24	4.93±1.04	0.92±0.17	3/5	8/9
U28+	1.60±1.08	0.70±0.90	2.80±1.90[a]	0.58±0.30[a]	0.5[c]	2/9[c]
M18−	1.73±1.35	2.37±2.52	4.95±1.48	6.75±1.94	0/5	0/9
M18+	2.00±1.50	1.73±1.63	1.87±1.17[b]	1.69±1.47[b]	0/5	0/9

Experiment 1: [a]$P=0.06$ (*t*-test); [b]$P=0.007$ (*t*-test); [c]$P=0.08$ (Fisher exact test). Experiment 2: [a]$P=0.011$ (*t*-test); [b]$P=0.000$ (*t*-test); [c]$P=0.008$ (Fisher exact test)

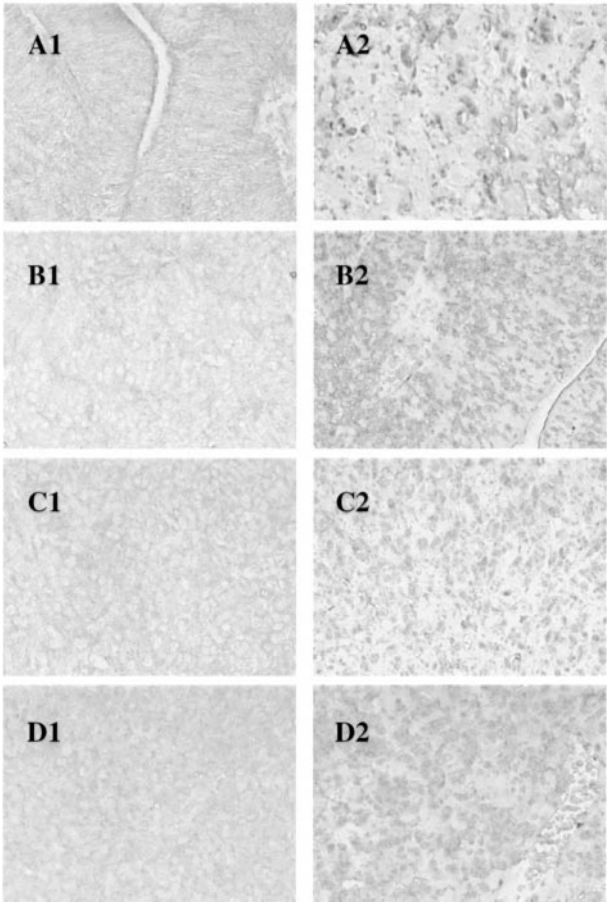

Figure 8 (A and B) IHC staining using a specific CL100 antibody of tumors formed in nude mice by the U28 cell line (20× magnification). (A1) U28− subcutaneous tumor. (A2) U28+ subcutaneous tumor. (B1) U28− intraperitoneal tumor. (B2) U28+ intraperitoneal tumor. (C and D) IHC staining of tumors formed in nude mice by the M18 inducible cell line (20× magnification). (C1) M18− subcutaneous tumor. (C2) M18+ subcutaneous tumor. (D1) M18− intraperitoneal tumor. (D2) M18+ intraperitoneal tumor

CL100 displayed reduced expression in epithelial ovarian cancers compared to IOSE and HOSE cells. CL100 is the human homolog of MKP-1 and is a nuclear DSP (Keyse and Emslie, 1992; Charles *et al*., 1992; Brondello *et al*., 1995; Sun *et al*., 1993; Alessi *et al*., 1993). DSPs differ from classical PTPs in their ability to dephosphorylate not only tyrosine but also serine/threonine residues in proteins. MKP-1 and CL100 were originally identified as ERK specific phosphatases, capable of dephosphorylating this MAPK (Sun *et al*., 1993; Alessi *et al*., 1993). However, in some mammalian cell lines the inactivation of this MAPK is too fast to indicate an involvement of CL100 in this process, and other phosphatases appear to be involved in the inactivation of MAPK (Alessi *et al*., 1995; Wu *et al*., 1994). Recent work has also implicated MKP-1 in the inactivation of the other members of the MAPK family, namely JNK and p38 in different model systems (Gupta *et al*., 1996; Chu *et al*., 1996).

While we documented a large differential expression of CL100 in ovarian cell lines, it was important to ensure that these differences did not simply reflect the immortalization of normal ovarian epithelial cells or were the result of the establishment of cancer cell lines. We analysed a large number of primary ovarian tissues (normal and malignant). High nuclear expression of CL100 was detected in normal ovarian epithelial cells. The expression of CL100 decreases from normal ovarian epithelium to early stage cancers and essentially disappears in advanced ovarian cancer. This finding partially parallels the expression patterns found in several other human cancers. In prostate, colon, and bladder, while overepxression of CL100/MKP-1 was observed in the early phases of carcinogenesis, there is a steady decrease in expression of MKP-1 with increasing stage of disease (Loda *et al*., 1996; Magi-Galluzzi *et al*., 1997). In contrast, there were detectable levels of MKP-1 observed in all stages of the breast cancer (Loda *et al*., 1996). However, the normal epithelial tissues examined did not express CL100 (Loda *et al*., 1996). Of further note, our immunostaining detected CL100 localized primarily to the nucleus while previous work analysing other human cancers has described primarily cytoplasmic staining (Loda *et al*., 1996). These differences may reflect pathologic differences in subcellular localization of CL100 in different tumors. It is unlikely that these differences in subcellular localization are the result of technical artifacts in the immunostaining, as the primary antibody used is specific for CL100/MKP-1 (as shown by the appropriate controls and also by Western blot) and previous studies finding a different subcellular localization have used the same antibodies and a similar

technique to the one used in this study (Loda *et al*., 1996). Nevertheless, some cytoplasmic staining of CL100 was also observed in a small percentage of ovarian cancer specimens. The downregulation of CL100 occurs predominantly as the tumor progresses from localized to advanced disease. This progression event corresponds with the important clinical transition in ovarian cancer from an essentially curable to incurable cancer (Ozols *et al*., 1997). The mechanism by which CL100 expression decreases remains to be determined. The induction of CL100 by hydrogen peroxide in two low expressing ovarian cancer cell lines suggests that the downregulation is a transcriptional event.

Our results show a decreased malignant potential of ovarian cancer cells expressing CL100. Cells with conditional expression of CL100 acquired a reversible loss of the transformed phenotype, with the acquisition of a flattened morphology that is characterized by a decreased motility. This report shows, for the first time, that restoring the expression of CL100 in ovarian cancer cells to the levels seen in normal ovarian cells has an inhibitory effect on cellular motility and growth. However, our *in vivo* data are most striking. Ovarian cancer cells with conditional expression of CL100 form fewer and smaller intraperitoneal tumors in nude mice. This is particularly relevant for a tumor that spends the majority of its life within the peritoneal cavity.

CL100 is a nuclear phosphatase whose known targets include the MAP kinases JNK and ERK (Sun *et al*., 1993; Alessi *et al*., 1993; Gupta *et al*., 1996; Chu *et al*., 1996) and in our transfectants the activities of these kinases were inhibited. Attenuation of signaling through MAPK pathways would alter gene expression. Expression of MKP-1 blocks the induction of DNA synthesis in quiescent REF52 fibroblasts by the V12 oncogenic mutant form of ras which is mediated by MAPK (Sun *et al*., 1994), and in fibroblasts MKP-1 also inhibits entry into S phase (Brondello *et al*., 1995; Noguchi *et al*., 1993). We demonstrated the down-regulation of cyclin D1 in CL100 expressing cells and that this regulation occurs at the AP-1 site in the cyclin D1 promoter, which is consistent with a decreased MAPK activity. These findings suggest that the cyclin D1 is likely involved in the growth effects induced by overexpression of CL100 in ovarian cancer cells as the changes in cyclin D1 expression correlate with the decreased growth rate observed. The mechanisms by which CL100 alters cellular morphology and motility are less clear but could involve the alterations of expression levels of proteins involved in those processes through attenuation of MAPK signaling. Of interest, treatment of the cell lines with PD98059 at 25 μM resulted in growth inhibition similar to CL100 expression (data not shown). However, inhibition of MEK-1/2/5 did not produce morphologic changes seen in the CL100 expressing clones. This suggests that ERK may affect cellular proliferation while JNK is more involved in cell morphology.

These findings provide a new insight into the biology of ovarian cancer. A model for ovarian cancer in which expression of CL100 acts as an important control in the acquisition of a full malignant and metastatic potential is proposed. Normal ovarian epithelial cells express high levels of CL100 perhaps as control to proliferative signals originating from the unique exposure of the cells to the peritoneal cavity. The decreased levels of CL100 found in early stage ovarian cancers may be sufficient to allow normal ovarian epithelial cells to proliferate in the initial stages of tumor formation. However, the complete loss of CL100 expression seen in advanced ovarian cancers would contribute to the acquisition of full metastatic potential.

Recent work from other laboratories has demonstrated the importance of the MAPK pathways in cancer cell growth and tumorigenesis (Hoshino *et al*., 1999; Sebolt-Leopold *et al*., 1999). It is known that many oncogenes can constitutively activate the MAPK pathway and that this inappropriate activation can lead to malignant transformation (Webb *et al*., 1998). Furthermore, activated MAPK or increased levels of MAPK expression have been found in a diverse array of human tumors such as breast, colon, lung and kidney cancers (Hoshino *et al*., 1999; Sebolt-Leopold *et al*., 1999). These observations have been exploited to create pharmacological inhibitors of this pathway, which could be of interest in a clinical setting. A recent report on a new specific inhibitor of MEK-1/2/5 (PD184352) has demonstrated that this approach is indeed effective in suppressing the growth of colon tumors *in vivo* (Sebolt-Leopold *et al*., 1999). In agreement with this data, our study shows that a decreased MAPK and JNK activity in ovarian cancer cells overexpressing CL100 correlates with the anti-proliferative effects of CL100 expression seen in these cells. As the presence of CL100 attenuates signaling through the MAPK pathways, all these observations point to the fact that ovarian epithelial cancer is a tumor that relies heavily on MAPK pathways and recent evidence, in addition to this report, supports this view (Hoshino *et al*., 1999; Sebolt-Leopold *et al*., 1999). Further, it has recently been shown that ovarian cancer presents frequent amplification of PIK3CA along with increased phosphatidylinositol 3-kinase (PI3K) activity (Shayesteh *et al*., 1999), suggesting a role for PIK3CA as an oncogene in ovarian cancer. It has also been demonstrated that activation of PI3K can lead to an increased ERK and JNK activity (Antonyak *et al*., 1998; Sajan *et al*., 1999). In ovarian cancer the expression of CL100 could act as an important control for increased MAPK signaling resulting from activated upstream pathways. Loss of CL100 expression would contribute to the transition from local to advanced ovarian tumors by allowing increased MAPK activation, and providing a unique and novel regulatory mechanism that is not present in other epithelial tumors.

In summary, our data strongly support the role of CL100 as a regulatory mechanism in the progression of ovarian carcinoma, and they shed new light in the biology of epithelial ovarian cancer. These findings also

open a new avenue for therapeutic intervention in these tumors.

Materials and methods

Plasmids and retrovirus production

pcDNA3-CL100 was prepared by subcloning a 1.2 kb *Sma* I/*Xho*I fragment from pMT2T-CL100 (a kind gift from K Kelly, NCI, Bethesda, MD, USA) into the *Eco*RV/*Xho*I site of pcDNA3 (Invitrogen).

Full length CL100 cDNA was cloned into a retroviral vector (pLRT) containing the two components of the reverse tetracycline-regulated (rtTA) system as described (Watsuji *et al*., 1997). UCI101 and A2780 cells were infected with the retrovirus pLRT-CL100 essentially as described (Watsuji *et al*., 1997).

Cell culture and cell culture assays

IOSE (immortalized ovarian surface epithelium) 80 and IOSE 120 are low passage normal ovarian surface epithelial cells which were immortalized with a SV40 large-T antigen-containing vector as described previously (Maines-Bandiera *et al*., 1992). These cells have an increased life span and express characteristics of normal ovarian surface epithelium. Given the difficulty in obtaining human normal ovarian surface epithelium, IOSE cells provide an *in vitro* model to study the biology of this epithelium.

The source of the ovarian carcinoma cell lines used in this study and the primary tumors they were derived from is as follows: AD10, UCI 101, UCI 107, A2780, OVCAR3, CaOv3, CP70, OVT2 A224, A364, A547 and SKOV3 were derived from papillary serous adenocarcinomas; OVCAR429 was derived from a serous cystoadenocarcinoma, and 222 was established from an endometriod adenocarcinoma. 222, AD10, UCI 101, UCI 107, and SKOV3 was kindly provided by Dr G Scott Rose, University of California, CA, USA; A2780, OVCAR3 and CaOv3 were obtained from the ATCC; cell line CP70 was provided by Dr Eddie Reed, NCI MD, USA; OVT2 was established in our laboratory; OVCAR429 was kindly provided by Dr David Spriggs, Memorial Sloan Kettering NY, USA; A224, A364, and A547 were provided by Dr Jacques DeGreves, Brussels, Belgium. Ovarian cell lines were cultured as described previously (Hendricks *et al*., 1997).

Stable transfection of ovarian cancer cell lines A2780 and UCI101 was carried out by electroporation using a Bio-Rad (Hercules, CA, USA) electroporator. Cells were transfected with either pcDNA3-CL100 or with pcDNA3 and selected (without trypsinization) with G418 500 μg/ml for 2–3 weeks. After selection, independent clones were isolated using cloning cylinders.

For oxidative stress assays, 2×10^6 cells were plated in 100 mm dishes and treated with 200 μM hydrogen peroxide for 30 min. The cells were then collected at different time points for the isolation of total RNA. Cellular proliferation assays were performed using a MTT (dimethyl thiozolyl-2′,5′-diphenyl-2-H-tetrazolium bromide) -based assay (Non radioactive proliferation assay, Promega Corp., Madison, WI, USA) as previously described (Sabichi *et al*., 1998). Anchorage independent growth was done as previously described (Sabichi *et al*., 1998). Colonies were scored with an Omnicon 3600 image analysis system (Imaging Products International, Inc. Chantilly, VA, USA) on day seven for A2780 stably transfected clones and on day 12 for UCI101 clones.

RNA isolation and Northern blot analysis

Total RNA was prepared from subconfluent cells using the standard guanidin isothiocyanate CsCl method. Ten micrograms RNA samples were electrophorised in 1% agarose gels containing formaldehyde and were transferred to Nytran N+ membranes (Schleicher and Schuell, Keene, NH, USA). Filters were incubated overnight with cDNA probes labeled with P^{32}-dCTP. The probes used were: a *Xho*I/*Eco*RI fragment (from pMT2-CL100, see below) of the human CL100 cDNA corresponding to part of the 3′ untranslated region or the full length CL100 cDNA. After an overnight hybridization at 60°C, blots were washed and exposed to XAR films (Kodak, Rochester, NY, USA). Signals were quantitated using a densitometer (Molecular Dynamics, Sunnyvale, CA, USA). To normalize for differences in RNA loading, all signals were adjusted based on the signal from the corresponding 28S ribosomal RNA band as visualized by ethidium bromide staining and UV illumination.

RT–PCR screening

RT–PCR was carried out using the conditions and primers essentially as described in Dayton and Knobloch (Dayton and Knobloch, 1997; Barnea *et al*., 1994). Specifically, for reverse transcription total cellular RNA was extracted from normal (IOSE 80, IOSE120) and malignant (AD10, CP70, 222) ovarian epithelial cell lines as described above. Complementary DNAs were prepared by random hexamer-primed reverse transcription (RT) of 0.5 μg of total RNA in a 20 μl reaction volume. A mixture of the RNA and 50 pmol random hexamers was heated to 75°C for 5 min and was rapidly cooled on ice. An RT master mix was then added such that the final concentrations were 50 mM KCl, 10 mM MgCl2, 20 mM Tris, 625 μM each of dATP, dCTP, dGTP, TTP, 2.5 mM dithiothreitol, 0.5 units rRNAsin/μl (Promega) and 2.5 units Superscript RT/μl (Gibco BRL). RT reactions were incubated at room temperature (25°C) for 15 min, at 42°C for 15 min, and at 55°C for 15 min. The RT was inactivated at 75°C for 15 min.

PCR amplification

A series of primers that correspond to specific PTPs were synthesized based on human sequence data when available. For those PTPs that had not been cloned from humans, the original primer sequences were chosen from the cDNA for the species of first cloning. Human primers were then based on the human sequences from the amplicons generated using the non-human primers. Primers were designed to yield amplicons ranging in length from 171 to 566 bp with temperatures for optimal PCR between 53.2 and 62.0°C. The characteristics of most of the PTPs primers used for these studies have been previously described (Dayton and Knobloch, 1997). The primer sets for the long and short extracellular forms of the receptor-like PTPs PTPζ, PTPζL and PTPζS (Barnea *et al*., 1994) included a common antisense primer (TTC TTG TGC TTG TTG TCT GGG TG) and unique sense primers (GAA TGA GAC TTC CAC AGA TTT CAG TTT and TGC CAC ATT ATT CTA CCT TTG CCT AC respectively). Primers for 10 additional PTPs and PTPs-like expressed sequence tags (ESTs–6 putative dual specificity phosphatases and a potential phosphatase

inhibitor) (PTP-TD14, PIR1, PRLCAAX3, PDSP1, PDSP2, PDSP3, PDSP4, PDSP5, PDSP6, and PDSPinh) will be described elsewhere (MA Dayton, manuscript in preparation). RT–PCR was done with template dilution and four sets of reactions with different annealing temperatures. The RT mixture was diluted 10–1000-fold in water so that amplicons of different abundance could be amplified in parallel with the same number of cycles. Based on the abundance of each amplicon in preliminary analysis, target sequences within 1 μl of the appropriate dilution of the cDNA reaction were amplified in 10 μl reactions containing 0.25 units of Taq, 2 pmol each of the sense and antisense primers in PCR buffer, 62.5 μM of each dNTP, and 0.05 μl [α-P32]dCTP. Control PCR reactions using no added DNA template and using no RT were done as sets after the cell line cDNA amplifications were complete. All PCR reaction components except for the primers and template were prepared as a master mix, which was subsequently aliquoted and overlaid with mineral oil. Both the master mix and the oil were added to the back inside of the PCR tube. All reactions were 'hot-started' as follows. One microliter each of the appropriate cDNA dilution and of a primer pair solution containing 2 pmols of each primer was deposited onto the front inside of the PCR tube, where they remained because of surface tension. The caps of the tubes were closed and then were placed into the thermal cycler. After heating the aliquoted master mixes to 80°C, the primers and template were mixed into the reaction solution. The samples were then briefly spun in a microcentrifuge to re-establish the oil layer on top. Amplification of each of the primer pair/template reactions was performed in parallel using the same master mix for each RT. Reactions were grouped into sets based on the optimum temperature for amplification–Tamp from 53.5–55.4°C were performed at 54°C, 55.5–57.4°C at 56°C, 57.5–59.4°C at 58°C, and 59.5–62.0°C at 60°C. The first two cycles of PCR consisted of denaturing at 97°C for 45 s, primer annealing at 54°C, 56°C, 58°C or 60°C for 300 s, and primer extending at 72°C for 60 s. An additional 28 cycles were completed under identical conditions except that the denaturation temperature was decreased to 94°C and the annealing time was decreased to 60 s.

Following electrophoresis through 1.5% Tris-Borate-EDTA (TBE) agarose gels, the amplicons were transferred by electroblotting to GeneScreen Plus nylon membranes (Dupont, Boston, MA, USA). DNA was fixed to the membranes by air-drying. The images were detected by PhosphorImager on a Molecular Dynamics PhosphorImager and were analysed by volume integration with the ImageQuant software. The expression levels for each of the PTPs were normalized to the G3PDH expression, taking into account the various dilutions of the RT made prior to the PCR.

Immunohistochemistry

Five micron formalin-fixed, paraffin-embedded tissue sections were used for immunohistochemical staining with specific rabbit polyclonal antibodies against MKP-1 (Santa Cruz Biotechnology, Santa Cruz, CA, USA) at a dilution of 1 : 50 utilizing standard techniques (Birrer *et al*., 1999). Positive controls of formalin-fixed paraffin-embedded sections included human tissues known to express high levels of CL100. The ovarian cancer cell line A224 with high endogenous levels of CL100 also served as positive control. Negative controls consisted of the incubation of serial (positive) ovarian tumor sections with an unrelated rabbit IgG polyclonal antibody. A previous immunohistochemical study using the same primary antibodies (at the same 1 : 50 dilution) to evaluate the expression of CL100 in other human tumors, also showed the specificity of the staining with these antibodies (Loda *et al*., 1996). Antigen retrieval was not performed in our study. In the previous study mentioned above, antigen retrieval did not reveal nuclear localization of CL100 in other human tumors (Loda *et al*., 1996). Staining was initially scored by both percentage of nuclei stained and intensity of the staining. Since the intensity of the staining was found to be similar in all specimens only the percentage of nuclei stained was reported. Results of the staining were reviewed independently without knowledge of the clinical data by two of the authors (RG Manzano and LM Montuenga) who scored the percentage of positive nuclei within tumors and in the normal ovarian surface epithelium. A score of 25% or higher was considered positive. Formalin-fixed, paraffin-embedded tissues were obtained from CHTN, National Naval Medical Center and Walter Reed Army Medical Center according to Institutional Review Boards approved protocols.

Western blotting analysis and kinase assays

Specific polyclonal antibodies against MKP-1 or cyclin D1 (both from Santa Cruz Biotechnology, Santa Cruz, CA, USA) were used as primary antibodies. A specific antibody against β-tubulin (Santa Cruz Biotechnology, Santa Cruz, CA, USA) was used as loading control on the same membrane used to assay for the expression of CL100 or cyclin D1. ERK-2, JNK-1 and p38 kinase activities were measured as previously described with minor modifications (Auer *et al*., 1998).

Immunofluorescence, F-Actin staining, and scanning electron-microscopy

Cells that had been grown on sterile coverslips were fixed with 3.7% formaldehyde in phosphate-buffered saline (PBS) for 10 min and then extracted with 0.2% Triton X-100 for 10 min at room temperature. After blocking nonspecific binding sites, anti-MKP1 antibody (Santa Cruz) was added to the coverslip and incubated for 1 h at 4°C. After the coverslip was washed, it was incubated at 4°C with fluorescein isothiocyanate (FITC)-conjugated goat anti-rabbit immunoglobulin (Molecular Probes). Finally, cells were stained with 0.4 μg/ml of DAPI (Sigma) for 10 min at room temperature. For actin staining, cells were processed as described above. Following fixation and extraction, one unit of rhodamine phalloidin (Molecular Probes) was added to the coverslip as recommended by the manufacturer and incubated at room temperature. Cells were stained with 0.4 μg/ml of DAPI (Sigma) for 10 min at room temperature. Cells were visualized on a Zeiss Axiovert microscope using a 63 $\times$ objective, and images were captured with an Optronics CCD camera.

For scanning electromicroscopy cells that had been grown on sterile coverslips were fixed with glutaraldehyde. After coating, cells were examined under scanning electron microscope.

Cell motility assay

FALCON cell culture inserts with an 8 μm pore-size PET membrane (Fisher Scientific) were coated with collagen 3 μg/ml for 2 h at 37°C, and placed into the wells of a 24-well plate containing 0.5 ml of RPMI supplemented with 0.5% serum and EGF at 10 nM. 350 μl of the cell suspension

(0.75×10^5 cells/ml in RPMI with 0.5% serum) was added to each insert. The plate was incubated for 24 h at 37°C and then the inserts were removed. Cells that had migrated through the insert and adhered to the bottom of the membrane were stained and then counted. Six high power fields randomly chosen were counted. The assay was performed in duplicate and repeated three times.

Luciferase assays

These assays were done as described with minor modifications using renilla as control for transfection efficiency (Tetsu and McCormick, 1999). All assays were done in triplicate and each experiment was repeated at least three times.

Nude mouse tumorigenicity

Nude mice were injected either subcutaneously or intraperitoneal with uninduced or induced (5 days) U28 or M18 cells. By using the tetracycline inducible system each clone serves as its own control to assure that the biologic effect seen is from the induced gene and not the result of clonal variation. A placebo or doxycycline pellet (Innovative Research of America, Sarasota, Florida, USA) was implanted in each mouse the day before the injection of the tumor cells. For the subcutaneous injections, 10^7 cells were injected. All mice that received the same cell line (whether induced or uninduced) were sacrificed the same day, when one or more developed a tumor volume of 2000 mm^3 or more as measured with a caliper. Tumors were removed and weighed. For the peritoneal injection, 2×10^7 cells were injected per mouse. Mice were sacrificed the same day after a 3-week period for M18 or after 6 weeks for U28. All macroscopic tumor was removed and weighed.

Statistical methods

Statistical analysis of the staining results was done using the χ^2 test and the Fisher exact test. Statistical analysis of the motility and of the *in vivo* study results was carried out using the student *t*-test (two tailed). The Fisher exact test was used to compare the statistical significance of the number of animals presenting ascites.

Acknowledgments
The ovarian cell lines used in this study were obtained as generous gifts from Dr Scott Rose (University of California, San Diego, CA, USA), Dr David Spriggs (Memorial Sloan Kettering Cancer Center, New York, NY, USA), Dr Jacques DeGreve (AZ-VUB-Oncologisch Centrum, Brussels, Belgium), and Dr Louis Dubeau (Norris Cancer Center, University of California, Los Angeles). The human cyclin D1 promoter plasmids were derived from fragments provided by Dr A Arnold and Dr R Pestell and constructed by Dr Osami Tetsu with Dr Frank McCormick. Protein lysates from HOSE cells were a kind gift of Dr Mok (Harvard University, Boston, MA, USA). We thank these individuals for their generous gifts. We thank Aaron Bell for his expert technical assistance. This work was supported in part by grants DK52825, CA88906 and DAMD-99-17-9426 to P Dent.

References

Alessi DR, Smythe C and Keyse SM. (1993). *Oncogene,* **8,** 2015–2020.
Alessi DR, Gomez N, Moorhead G, Lewis T, Keyse SM and Cohen P. (1995). *Curr. Biol.,* **5,** 283–295.
Antonyak MA, Moscatello DK and Wong AJ. (1998). *J. Biol. Chem.,* **273,** 2817–2822.
Auer KL, Park JS, Seth P, Coffey RJ, Darlington G, Abo A, McMahon M, Depinho RA, Fisher PB and Dent P. (1998). *Biochem. J.,* **336,** 551–560.
Barnea G, Grumet M, Milev P, Silvennoinen O, Levy JB, Sap J and Schlessinger J. (1994). *J. Biol. Chem.,* **269,** 14349–14352.
Birrer MJ, Hendricks D, Farley J, Sundborg MJ, Bonome T, Walts MJ and Geradts J. (1999). *Cancer Res.,* **59,** 5270–5274.
Brondello JM, McKenzie FR, Sun H, Tonks NK and Pouyssegur J. (1995). *Oncogene,* **10,** 1895–1904.
Charles CH, Abler AS and Lau LF. (1992). *Oncogene,* **7,** 187–190.
Chu Y, Solski PA, Khosravi-Far R, Der CJ and Kelly K. (1996). *J. Biol. Chem.,* **271,** 6497–6501.
Cliby W, Ritland S, Hartmann L, Dodson M, Halling KC, Keeney G, Podratz KC and Jenkins RB. (1993). *Cancer Res.,* **53,** 2393–2398.
Dayton MA and Knobloch TJ. (1997). *Recept. Signal Transduct.,* **7,** 241–256.
Devesa SS, Blot WJ, Stone BJ, Miller BA, Tarone RE and Fraumeni Jr JF. (1995). *J. Natl. Cancer Inst.,* **87,** 175–182.
Dodson MK, Hartmann LC, Cliby WA, DeLacey KA, Keeney GL, Ritland SR, Su JQ, Podratz KC and Jenkins RB. (1993). *Cancer Res.,* **53,** 4456–4460.
Fischer EH, Charbonneau H and Tonks NK. (1991). *Science,* **253,** 401–406.
Greenlee RT, Hill-Harmon MB, Murray T and Thun M. (2001). *Ca-A Cancer Journal for Clinicians,* **51,** 15–36.
Gupta S, Barrett T, Whitmarsh AJ, Cavanagh J, Sluss HK, Derijard B and Davis RJ. (1996). *EMBO J.,* **15,** 2760–2770.
Hendricks DT, Taylor R, Reed M and Birrer MJ. (1997). *Cancer Res.,* **57,** 2112–2115.
Hoshino R, Chatani Y, Yamori T, Tsuruo T, Oka H, Yoshida O, Shimada Y, Ari-i S, Wada H, Fujimoto J and Kohno M. (1999). *Oncogene,* **18,** 813–822.
Keyse SM and Emslie EA. (1992). *Nature,* **359,** 644–647.
Loda M, Capodieci P, Mishra R, Yao H, Corless C, Grigioni W, Wang Y, Magi-Galluzzi C and Stork PJ. (1996). *Am. J. Pathol.,* **149,** 1553–1564.
Magi-Galluzzi C, Mishra R, Fiorentino M, Montironi R, Yao H, Capodieci P, Wishnow K, Kaplan I, Stork PJ and Loda M. (1997). *Lab. Invest.,* **76,** 37–51.
Maines-Bandiera SL, Kruk PA and Auersperg N. (1992). *Am. J. Obstet. Gynecol.,* **167,** 729–735.
Neel BG and Tonks NK. (1997). *Curr. Opin. Cell Biol.,* **9,** 193–204.
Noguchi T, Metz R, Chen L, Mattei MG, Carrasco D and Bravo R. (1993). *Mol. Cell Biol.,* **13,** 5195–5205.
Ozols RF, Rubin SC, Thomas G and Robboy S. Epithelial ovarian cancer. In W.J. Hoskins, C.A. Perez and R.C. Young (eds.), Principles and Practice of Gynecologic Oncology, Philadelphia: Lippincott-Raven Publishers, 1997. pp. 919–986.

Sabichi AL, Hendricks DT, Bober MA and Birrer MJ. (1998). *J. Natl. Cancer Inst.,* **90,** 597–605.
Sajan MP, Standaert ML, Bandyopadhyay G, Quon MJ, Burke Jr TR and Farese RV. (1999). *J. Biol. Chem.,* **274,** 30495–30500.
Sebolt-Leopold JS, Dudley DT, Herrera R, Van Becelaere K, Wiland A, Gowan RC, Tecle H, Barrett SD, Bridges A, Przybranowski S, Leopold WR and Saltiel AR. (1999). *Nat. Med.,* **5,** 810–816.
Shayesteh L, Lu Y, Kuo WL, Baldocchi R, Godfrey T, Collins C, Pinkel D, Powell B, Mills GB and Gray JW. (1999). *Nat. Genet.,* **21,** 99–102.
Sun H, Charles CH, Lau LF and Tonks NK. (1993). *Cell,* **75,** 487–493.
Sun H, Tonks NK and Bar-Sagi D. (1994). *Science,* **266,** 285–288.
Tetsu O and McCormick F. (1999). *Nature,* **398,** 422–426.
Tonks NK and Neel BG. (1996). *Cell,* **87,** 365–368.
Watsuji T, Okamoto Y, Emi N, Katsuoka Y and Hagiwara M. (1997). *Biochem. Biophys. Res. Commun.,* **234,** 769–773.
Webb CP, Van Aelst L, Wigler MH and Woude GF. (1998). *Proc. Natl. Acad. Sci. USA,* **95,** 8773–8778.
Wiener JR, Kassim SK, Yu Y, Mills GB and Bast Jr RC. (1996). *Gynecol. Oncol.,* **61,** 233–240.
Wu J, Lau LF and Sturgill TW. (1994). *FEBS Lett.,* **353,** 9–12.